Chapter 8
Studying the Role of Gas Bubbles on Air-Sea Gas Transfer Using Computer Models

Jun-Hong Liang

Abstract Oceanic gas bubbles, the building blocks of whitecaps, play important roles in air-sea gas transfer at moderate to high wind speed when wave breaking and bubble formation are frequent. This review focuses on the development of computer models, usually constrained by laboratory and field observation, to improve the qualitative and quantitative understanding of bubble-mediated air-sea gas transfer. The construction of bubble models, the coupling of bubble models with other ocean models, examples of their application and major findings from existing bubble modeling studies are discussed and summarized.

8.1 Introduction

Oceanic gas bubbles, visually identified as whitecap at the ocean surface because of their distinctly different optical property from seawater, influences the properties of both sides of the ocean-atmosphere interface. One of the disciplines that bubbles play an important role in is air-sea gas transfer. Air-sea gas transfer modulates dissolved gas concentration in the ocean surface mixed layer and the cycling of chemical elements between the ocean and the atmosphere (e.g., Hamme et al. 2019). Air-sea gas transfer at low wind speeds ($U_{10} < \sim 7$ m/s) is relatively well understood thanks to a series of theoretical (e.g., Liss and Slater 1974), laboratory (e.g., Broecker et al. 1978) and in situ studies (e.g., Wanninkhof et al. 1993; Asher 1997). The ocean under these wind speeds is unbroken though possibly wavy, and gases diffuse in and out of the ocean through the ocean-atmosphere interface. The gas transfer rate for this regime is proportional to wind speed. In contrast, air-sea gas exchange at moderate to extreme wind speeds ($U_{10} > \sim 7$ m/s) is more challenging to quantify. At these wind speeds, ocean surface gravity waves break and the breaking waves entrain air bubbles into the ocean (e.g., Monahan and Torgersen 1991; Farmer et al. 1993). Gas transfer occurs not only at the ocean surface, but also

J.-H. Liang (✉)
Department of Oceanography and Coastal Sciences & Center for Computation and Technology, Louisiana State University, Baton Rouge, LA, USA
e-mail: Jliang@lsu.edu

P. Vlahos (ed.), *Recent Advances in the Study of Oceanic Whitecaps*,
https://doi.org/10.1007/978-3-030-36371-0_8

between gas bubbles inside the ocean surface mixed layer and the surrounding water. The significance of gas bubbles in air-sea gas transfer generally increases with wind speed since wave breaking occurs more frequently and turbulence that traps bubbles becomes more energetic. Under hurricane winds, the contribution from bubbles is dominant (D'Asaro and McNeil 2007; McNeil and D'Asaro 2007). Bubbles contribute to the total air-sea gas flux for most gases in two ways (e.g., Woolf 1997): (1) the enhancement of the total gas transfer rate and (2) surface bubble-induced equilibrium supersaturation. Bubbles provide a pathway in addition to the ocean surface for air-sea gas transfer; gas transfer rate is, therefore, larger with bubbles than without bubbles. Gases can dissolve from bubbles at supersaturated conditions, caused by the surface tension and hydrostatic pressure on bubbles. Intuitively, gases can dissolve into water that is 200% saturated when a bubble is deeper than 10 m. When the total gas flux is zero, the surface ocean is supersaturated with surface outgassing balanced by interior dissolution through bubbles. For polar gases such as DMS that are more prone to stay at the bubble-water interface than the aqueous or gas phase alone, bubbles enhance their effective solubility (Vlahos and Monahan 2009; Vlahos et al. 2011). Besides directly transferring gases through their interface, bubbles also enhance surface transfer rate when they burst by disrupting the diffusive sublayer.

Mathematically, the total air-sea gas flux F, including the contribution from bubbles, is expressed as (e.g., Woolf 1997),

$$F = (k_s + k_b)[SP_{atm}(1 + \Delta_b) - C_w] \tag{8.1}$$

where k_s and k_b are the gas transfer rate at the ocean surface and bubble-water interface, respectively; S is gas solubility; P_{atm} is atmospheric pressure; Δ_b is bubble-induced equilibrium supersaturation defined as the relative deviation of dissolved gas concentration from saturation concentration due to bubbles; C_w is dissolved gas concentration. The bubble-enhanced gas transfer rate is either explicitly or implicitly in many widely used gas flux parameterizations (e.g., Wanninkhof et al. 2009; Fairall et al. 2011). Bubble-induced equilibrium supersaturation Δ_b, however, is not commonly included. Recently, the importance of Δ_b has been realized as saturation anomaly influences the estimate of other biogeochemical processes, such as biological production and denitrification, using dissolved gas measurements (e.g., Emerson and Bushinsky 2016; Nicholson et al. 2016). Quantification of Δ_b is very challenging as direct measurement of gas flux across bubble-water interface in the ocean is impossible. Currently, two approaches are used to estimate Δ_b. The first approach utilizes observations of the dissolved gas saturation anomaly (e.g., Stanley et al. 2009; Vagle et al. 2010). By subtracting the contribution to the gas saturation anomaly by processes other than bubbles, the effect by bubble-mediated gas flux is quantified. The second approach directly calculates the gas flux through bubbles using bubble fields. Quantitative observation of bubbles in the ocean surface boundary layer is very limited (e.g., Farmer et al. 1998), and it is particularly challenging at high wind speed when bubble-mediated gas transfer is important. The approach is therefore achieved by using calculated bubble fields, usually constrained by the

limited observations (e.g., Woolf and Thorpe 1991). This review focuses on the use of a computer model that generates subsurface bubble fields to derive bubble-mediated air-sea gas flux.

8.2 Bubble Modelling

8.2.1 Bubble Processes

A bubble model needs to simulate all important bubble processes that are reviewed in this subsection. The majority of gas bubbles form during the breaking of surface gravity waves, although they can also be generated by the impact of raindrops at the ocean surface, from seafloor gas vents, and through biological processes such as photosynthesis that releases gases. After their formation, gas bubbles rise due to their own buoyancy. At the same time, the energetic turbulent ocean surface boundary layer currents compete with the buoyancy of bubbles to keep them suspended in the water column. While in the water column, gas bubbles exchange gases with the surrounding water. They also change size when they exchange gas with the surrounding water and when they move up and down in the water column leading to the change in hydrostatic pressure. Large, fast-rising bubbles have a relatively short life in the water column and eventually burst at the ocean surface. Small, slow-rising bubbles are able to suspend in the water for a long period so that gases in them completely dissolve in the water. The fate of bubbles is important for the purpose of bubble-mediated air-sea gas transfer. Intuitively, the amount of gas dissolving from completely dissolved bubble equals to the amount of gases in those bubbles, while the amount gas dissolving from partially dissolved bubbles are controlled by a number of factors such as gas solubility, gas diffusivity, and the life span of those bubbles, in addition to the amount of gas in those bubbles. Theoretically, it can be shown that k_b is only determined by flux through the relatively large, partially dissolved bubbles, while Δ_b is controlled by flux through all bubbles including both the completely and partially dissolved bubbles (e.g., Liang et al. 2013) (Fig. 8.1).

8.2.2 Construction of a Bubble Model

There are two types of bubble models: an Eulerian bubble concentration model and a Lagrangian bubble model. In the Eulerian bubble concentration model, bubble concentrations at each spatial location (computational grids) are calculated. In a Lagrangian bubble model, a large amount of Lagrangian particles, each representing a certain number of actual bubbles, are traced. The two types of models are separately reviewed:

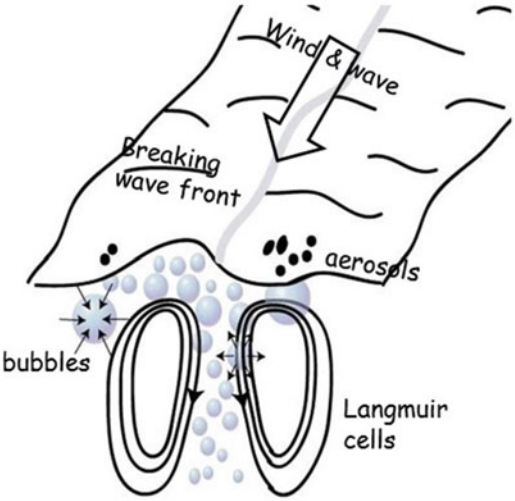

Fig. 8.1 A schematic showing processes related to oceanic bubbles

8.2.2.1 Eulerian Model

For the accurate calculation of gas flux through bubbles, bubble concentration field is modeled as,

$$\begin{aligned}\frac{\partial n_j(\mathbf{x}, r, t)}{dt} = & advection + diffusion \\ & + buoyant\ \ rising \\ & + gas\ exchange\ with\ \ surrounding\ water \\ & + bubble\ size\ change \\ & + bubble\ formation\ \ under\ breaking\ waves \\ & + bubble\ \ bursting\end{aligned} \tag{8.2}$$

where n_i is the concentration density of gas i in bubbles of radius r at spatial location $\mathbf{x}$ and time t. Bubble number density is diagnosed from n_i using the ideal gas law. The detailed mathematical expressions for the right-hand-side RHS terms can be found in Equations (1) to (5) in Liang et al. (2011). The first two terms, i.e., turbulent advection and diffusion, are based on fluid dynamical principles. The rest of the RHS terms related to bubble physics and dynamics come from many theoretical and experimental studies (e.g., Thorpe 1982; Lamarre and Melville 1991; Deane and Stokes 2002). The equation requires inputs of water velocity, dissolved gas concentrations in the surrounding water, and other parameters related to gases such as diffusivity and solubility.

There are here a couple of differences from bubble models used to study bubbles in the surf zone or in a laboratory flume (e.g., Shi et al. 2010). First, gas dissolution included in Eq. (8.2) is neglected in surf zone bubble models. It is shown in Liang

et al. (2012) that gas dissolution is the dominant factor shaping the distribution of bubbles in an oceanic surface boundary layer except very close to the surface where breaking waves actively entrain bubbles. Secondly, the amount of individual gases in bubbles is explicitly prognostic in Eq. (8.2) while bubble number density is modeled in surf zone bubble models. The gas fraction in bubbles dynamically evolves using Eq. (8.2). This is important to accurately diagnose gas flux through bubbles. Because different gases have different solubility, the fraction of a gas differs from the atmospheric fraction of the gases after bubble formation. It is demonstrated in Liang et al. (2012) that the averaged fraction of O_2 goes from approximately 0.21 at the surface to about 0.15 at 15 m depth under a 10-m wind speed of 20 m/s. Assuming a constant gas fraction based on atmospheric gas composition would lead to an underestimate of gas flux from the less soluble gas N_2 and overestimate of gas flux for more soluble O_2.

The biggest appeal of an Eulerian bubble model is the relatively straightforward coupling with a hydrodynamic model. Equation (8.2) can be discretized and solved in the same spatial computing grid as for the hydrodynamic model and n_j is conveniently added as an additional tracer in the model. There are a few limitations associated with the numerical solution of an Eulerian bubble model. First, Eq. (8.2) includes an advection term and its numerical solution cannot avoid the inherent, spurious diffusive (smoothing) and dispersive (oscillating) errors. Secondly, Eq. (8.2) has to be solved for different gas components in different size bins. For example, 3 gases and 200 size bins are used in Liang et al. (2011) to simulate bubbles under an individual breaking wave, implying that Eq. (8.2) is solved 600 times at each spatial location $\mathbf{x}$. Furthermore, when bubbles are simulated in the ocean surface boundary layer, the vertical extent of the computing grid has to be 2 to 3 times the boundary layer depth and is usually greater than 100 m although bubbles are only in the upper 10 or 20 m of the water column. In Liang et al. (2013), 2 gases and 17 size bins are used and the authors were able to carry out bubble flow simulations for about a half day. Finally, the separation of completely and partially dissolved bubbles is ambiguous in an Eulerian bubble model because we are not able to follow individual bubbles in an Eulerian bubble concentration model. Since the separation is crucial in a model for gas flux through bubbles based on first principles, the ratio of the two types of bubbles is diagnosed using the gas flux ratio in Liang et al. (2013).

8.2.2.2 Lagrangian Bubble Model

In a Lagrangian bubble model, the location ($\mathbf{x}$), gas contents (n_j with subscript j indicates gas type, e.g., j = 1 for N_2, and j = 2 for O_2), and size (r) of each Lagrangian particle are solved,

$$\frac{d\mathbf{x}}{dt} = \mathbf{u} \tag{8.3a}$$

$$\frac{dn_j}{dt} = f\left(r, z, c_j, S_j, D_j\right) \tag{8.3b}$$

$$\frac{dr}{dt} = f\left(\frac{dn_j}{dt}, w\right) \tag{8.3c}$$

In Eq. (8.3b), z is the vertical location of the Lagrangian particle; c_j, S_j, and D_j, is the dissolved concentration in the surrounding water, the solubility, and the diffusivity of gas j, respectively. Particle velocity (**u**) includes the effect of current, wave, and its own buoyancy that is size dependent. Ideally, each Lagrangian particle represents one gas bubble, but that is currently impossible because there are numerous bubbles in the ocean and computing power is limited. In actual simulations, each Lagrangian particle represents a large number of actual bubbles. Following the tradition in Lagrangian modeling of atmospheric cloud droplets where a Lagrangian particle is called a "super-droplet", the Lagrangian particles are called "superbubbles" in Liang et al. (2017). In Woolf and Thorpe (1991) where Langmuir circulations are represented by steady circulation cells, 5000 superbubbles were used. In Liang et al. (2017) where the ambient current is fully turbulent and unsteady, 8 million superbubbles were used.

A Lagrangian bubble model has the following advantages over an Eulerian bubble concentration model. Physically, a Lagrangian model allows straightforward separation of completely and partially dissolved bubbles since the fate of individual bubbles is tracked. Numerically, the Lagrangian model is a set of ordinary differential equations, whose numerical solutions are straightforward, without nonphysical effects associated with the dispersive and diffusive errors inherent to the numerical solutions of advection-diffusion equations in an Eulerian model. Computationally, computing power is allocated only to locations where bubbles are abundant, while bubble concentrations are calculated at each grid point for each size in an Eulerian coordinate system, even at depths where bubbles seldom reach and for sizes of few bubbles. The processor to compute a Lagrangian particle is the one that computes turbulent flow at the location of the particle. Buoyant particles are unevenly distributed in space, particularly in wave-driven Langmuir circulations, therefore computing loads are also unevenly distributed among processors. Our experience is that this increase in computing time due to heterogeneity is moderate and we are able to simulate bubbly flows for a two-week period in Liang et al. (2017). However, a Lagrangian model is less straightforward to implement in a parallel computing framework. A large number of Lagrangian particles are required to represent a field in the space.

8.2.2.3 Coupling with Hydrodynamic Model and Dissolved Gas Model

Bubble models require information about ambient current, temperature, and dissolved gas concentration. In early bubble modeling studies, due to insufficient knowledge of turbulent flows in the ocean surface boundary layer and limited

computing power, the effect of turbulence on bubbles is either neglected (Memery and Merlivat 1985), or by a pair of steady counter-rotating circulation cells mimicking Langmuir circulation (e.g., Woolf and Thorpe 1991). Dissolved gas concentration is set to a constant in those studies. In the past two decades when computation-expensive data-intensive parallelized computer models are able to resolve water turbulence, the concurrent simulation of turbulent flow and bubble fields becomes possible. Direct numerical simulation (DNS), where all water motions are resolved, has been used to simulate the evolution of bubbly flows under breaking waves in surf zones (e.g., Derakhti and Kirby 2014; Deike et al. 2016). However, DNS of the ocean surface boundary layer which is much deeper than the surf zone is still formidable in the foreseeable future because the ocean surface boundary layer is highly turbulent requiring a large number of grid points to resolve motions at all scales. Large eddy simulation (LES), where the majority of the energetic turbulent flows is simulated and the unresolved motions have little effect on resolved motions, is the popular approach to simulate boundary layer turbulence.

In the past few years, we coupled bubble models, first an Eulerian bubble concentration model (Liang et al. 2012) and later a Lagrangian bubble model (Liang et al. 2017) in a paralleled LES model for ocean surface boundary layer flows. The LES model we used is the National Center for Atmospheric Research Large Eddy Simulation (NCAR-LES) model (e.g., McWilliams et al. 1997). It is considered a state-of-the-art model for turbulent flows in the ocean surface boundary layer, and has been applied to study ocean turbulent flows under a variety of surface meteorological conditions and lateral forcing (See Sullivan and McWilliams 2010 and references therein). In a recent study (Liang et al. 2017), we demonstrated the use of the model to reproduce the observed concurrent evolution of the hydrodynamics, bubbles, and dissolved gases. The coupling between different models is illustrated in Fig. 8.2.

8.3 Studying Bubble-Mediated Gas Transfer Using a Computer Model

Four studies using numerical models to study bubble-mediated gas transfer are reviewed in this section in chronological order.

8.3.1 The Study of Merlivat and Memery (Memery and Merlivat 1985) (Hereafter MM85)

In MM85, bubbles are modeled as Lagrangian particles (superbubbles). In an era without advanced knowledge of boundary layer currents, superbubbles of diameter from 50 μm to 2000 μm are assumed to rise at their terminal velocity in quiescent

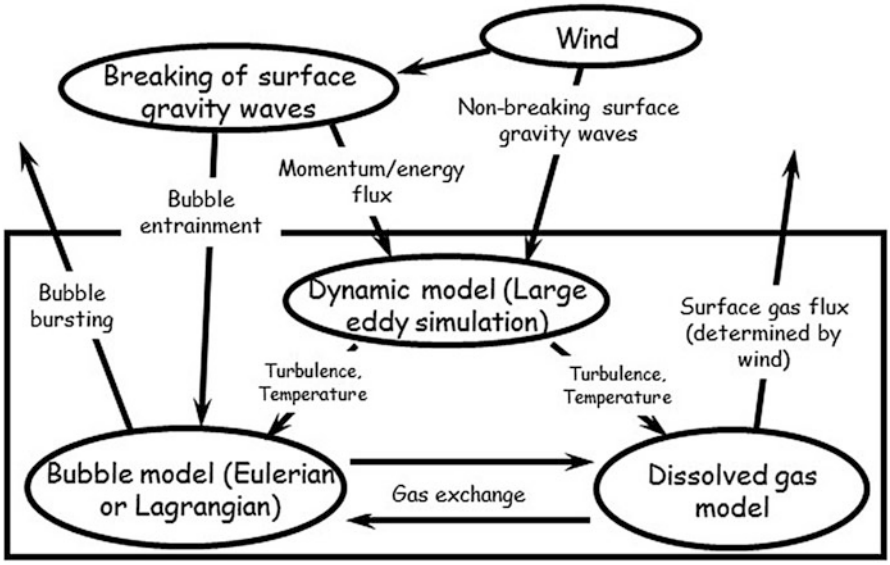

Fig. 8.2 A schematic showing the coupled hydrodynamic-bubble-gas model

water after their release in the ocean. Gas flux from each superbubble during its whole life in the water column ($q(r_0, z_0)$ with r_0 the initial size and z_0 the depth of entrainment by breaking wave) is computed. Because the evolution of each superbubble is deterministic, the gas flux through bubbles (F_b) is then calculated as,

$$F_b = \iint S(r_0, z_0) q(r_0, z_0) dr dz \tag{8.4}$$

where $S(r_0, z_0)$ is the bubble source function and the mean observed subsurface bubble distribution function was used by the authors. The use of mean subsurface bubble distribution as a bubble source function is not accurate, but was the best the authors could do at that time. The study draws some useful qualitative conclusions and new insights on how bubble-mediated gas transfer is influenced by gas solubility, gas diffusivity, and surfactants.

8.3.2 *The Study of Woolf and Thorpe (1991) (Hearafter WT91)*

Woolf and Thorpe (1991) also utilized a Lagrangian bubble model, similar to MM85, but made a few important improvements to the approach. In WT91, Langmuir circulations were included, as steady and counter-rotating circulation cells and background turbulence were modeled as isotropic random displacement determined

by diffusivity that is assumed uniform in the water column. The mean observed subsurface bubble distribution was used to tune the initial bubble size distribution. Furthermore, updated formulas for bubble and gas physics were used. Since bubble evolution is no longer deterministic due to turbulence, bubble gas flux is computed using simulated equilibrium bubble fields ($\Phi(r,\mathbf{x})$ with r the bubble size and $\mathbf{x}$ the bubble location) as,

$$F_b = \iint \frac{dn_j}{dt} \Phi(r, \mathbf{x}) dr d\mathbf{x} \tag{8.5}$$

Using the simulated bubble solutions, the authors are the first to propose parameterization for bubble-induced supersaturation and the parameterization has been shown to produce a reasonable agreement with dissolved gas measurements in a global model (Liang et al. 2013). They also suggested that gas flux depends on the saturation level of the most abundant gases including O_2 and N_2.

8.3.3 The Study of Liang et al. (2013) (Hearafter L13)

L13 fitted a parameterization for bubble gas flux based on simulated bubble fields in Langmuir turbulence driven by waves in equilibrium with the wind. The bubble fields were simulated with an Eulerian bubble concentration model (Eq. 8.2) and the bubble-mediated gas flux (F_b) is calculated the same way as in WT91 (Eq. (8.5)). Similar to some previous parameterization derived from observations (e.g., Stanley et al. 2009; Nicholson et al. 2011), the parameterization by L13 separates completely and partially dissolved bubbles indirectly through analyzing the gas flux ratio between O_2 and N_2. It was also demonstrated that bubble-induced equilibrium supersaturation (Δ_b) is temperature dependent and is larger at lower temperatures because diffusive gas flux at the ocean surface that offsets gas injection through bubbles is slower at lower temperatures. The authors also compared existing parameterizations that include Δ_b and show that huge uncertainty exists in those parameterizations. For example, bubble-induced supersaturation for N_2 spans the range from ~ 2% to more than 12% among different parameterizations.

The parameterizations were then tested in a global ocean transport model. Although bubbles only stay in the upper ocean for a short period of time, they set the near-surface dissolved gas concentration as a boundary for ocean ventilation and have non-negligible effects in the deep ocean. For example, L13 showed that bubbles at the near-surface ocean contribute more than 1% of the saturation level for Argon in the abyssal ocean and are crucial for accurately simulating deep-water gas concentration.

8.3.4 The Study of Liang et al. (2017) (Hearafter L17)

L17 applied a coupled hydrodynamic-bubble-dissolved gas model to study the evolution of the ocean environment and dissolved gases under a winter storm with wind speeds up to 20 m/s at ocean station Papa, where concurrent, relatively high-resolution (hourly or three-hourly), observations at both sides of the ocean-atmosphere interface including wind, buoyancy fluxes, wave, temperature, salinity, and dissolved gas concentrations are available. While the model-data comparison in L13 is for long-term means, the model-data comparison in L17 is for a transient synoptic event.

An instantaneous snapshot of subsurface bubble distribution (Fig. 8.3) shows that bubbles are mixed to more than 20 m during the peak wind of 20 m/s or so. The model reproduces the transient evolution of both observed O_2 and N_2 in the mixed layer when bubbles are considered. Without bubbles, the dissolved concentrations of both gases are underestimated. L17 also showed that sea state is an important parameter for bubble-mediated air-sea gas transfer, consistent with some other recent studies (e.g., Brumer et al. 2017; Deike and Melville 2018). When waves are less developed, there are fewer but larger breaking waves, leading to deeper bubble entrainment and larger gas fluxes through bubbles. At the same wind speed, gas flux through bubbles when the wind is strengthening, and the wave is less developed, can be twice as large as that when the wind is weakening.

8.4 Outlook

Computer models have improved our quantitative and qualitative understanding of bubble-mediated air-sea gas transfer. With the many data obtained recently and in the near future (see other chapters of this book), and the continued advancement in supercomputers, bubble models can be further improved by more detailed simulations of bubble and gas processes, such as entrainment under breaking waves and gas dissolution that are currently highly parameterized. Furthermore, existing bubble modeling studies are all for bubbles under the exclusive influence of boundary layer turbulence. Bubbles have been observed to reach tens of meters (Baschek et al. 2006) and are expected to contribute to the aeration of the water column in those scenarios that deserve more studies.

In addition to their significant role in air-sea gas transfer, bubbles also play important roles in other disciplines in oceanography, ocean sensing and earth science. For example, their optical and passive acoustical footprints are used to study and quantify dynamic processes, such as breaking waves (e.g. Melville and Matusov 2002) and turbulent mixing (e.g., Wang et al. 2016) in the upper ocean. Active noise levels during bubble formation were used to infer strong wind speeds (e.g., Zhao et al. 2014). In addition to gas transfer in the surface ocean, bubbles carry gases such as methane from the seafloor through the water column to the atmosphere

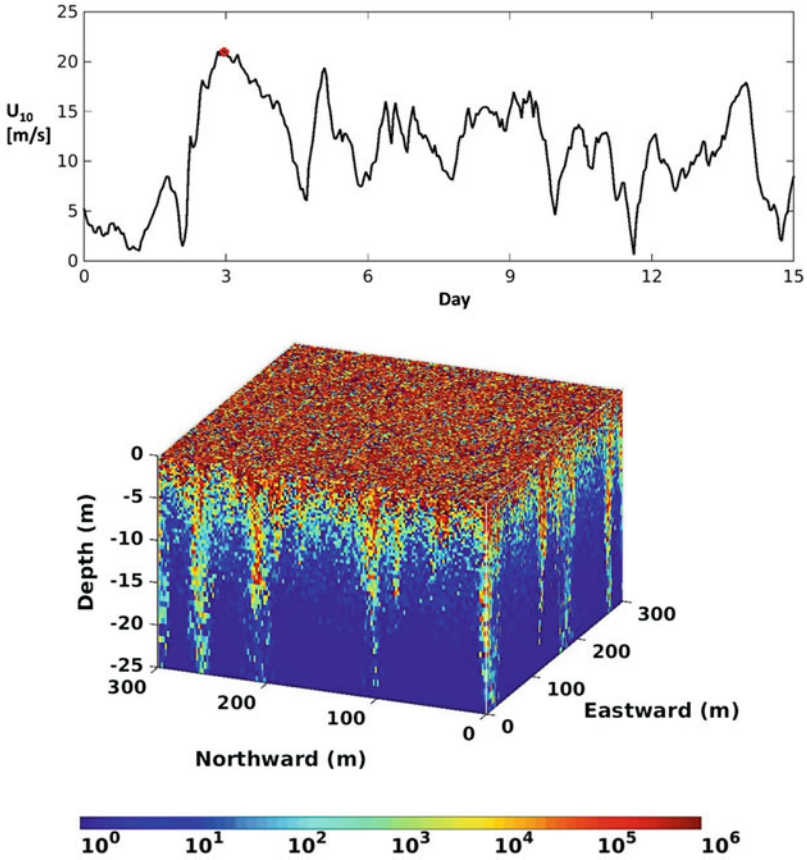

Fig. 8.3 Time series of wind speed during the period of simulation with day 0 corresponding to the start of Nov. 14th 2011 GMT (upper panel), and simulated bubble number density during peak wind denoted by a red circle in the upper panel. See Liang et al. (2017) for detailed description of the model configuration and other model results

(e.g., Leifer and Patro 2002). When bubbles burst, they contribute to aerosol production (Monahan et al. 1986) that leads to the formation of marine clouds. Finally, artificially generated bubbles have been proposed as a geoengineering approach to reduce night-time bottom water acidification in shallow water (Koweek et al. 2016). The use of bubble models is expected to improve the qualitative and quantitative understanding of these subjects.

Acknowledgement The author would like to acknowledge funding support from the National Science Foundation through grant OCE-1521018 and OCE-1558317. Computation in this study was carried out on high-performance supercomputing facilities at Louisiana State University and at the National Center for Atmospheric Research.

References

Asher, W. (1997). The sea-surface microlayer and its effect on global air-sea transfer. In P. S. Liss & R. Duce (Eds.), *The sea surface and global change* (pp. 251–285). A: Cambridge University Press.

Baschek, B., Farmer, D. M., & Garrett, C. (2006). Tidal fronts and their role in air-sea gas exchange. *Journal of Marine Research, 64*, 483–515.

Broecker, H. C., Petermann, J., & Siems, W. (1978). Influence of wind on CO2 exchange in a wind-wave tunnel, including effects of monolayers. *Journal of Marine Research, 36*(4), 595–610.

Brumer, S., Zappa, C., Blomquist, B., Fairall, C., Cifuentes-Lorenzen, A., Edson, J., et al. (2017). Wave-related Reynolds number parameterizations of CO2 and DMS transfer velocities. *Geophysical Research Letters, 44*, 9865–9875.

D'Asaro, E., & McNeil, C. (2007). Air-sea gas exchange at extreme wind speeds measured by autonomous oceanographic floats. *Journal of Marine Systems, 66*, 92–109.

Deane, G. B., & Stokes, M. D. (2002). Scale dependence of bubble creation mechanisms in breaking waves. *Nature, 418*, 839–844.

Deike, L., & Melville, W. K. (2018). Gas transfer by breaking waves. *Geophysical Research Letters, 45*, 10482–10492.

Deike, L., Melville, W. K., & Popineta, S. (2016). Air entrainment and bubble statistics in breaking waves. *Journal of Fluid Mechanics, 801*, 91–129.

Derakhti, M., & Kirby, J. T. (2014). Bubble entrainment and liquid-bubble interaction under unsteady breaking waves. *Journal of Fluid Mechanics, 761*, 464–506.

Emerson, S., & Bushinsky, S. (2016). The role of bubbles during air-sea gas exchange. *Journal of Geophysical Research, Oceans, 121*, 4360–4376.

Fairall, C. W., Yang, M., Bariteau, L., Edson, J. B., Helmig, D., McGillis, W., Pezoa, S., Hare, J. E., Huebert, B., & Blomquist, B. (2011). Implementation of the Coupled Ocean-Atmosphere Response Experiment flux algorithm with CO2, dimethyl sulfide, and O3. *Journal of Geophysical Research, 116*, C00F09.

Farmer, D. M., McNeil, C. L., & Johnson, B. D. (1993). Evidence for the importance of bubbles in increasing air-sea gas flux. *Nature, 361*, 620–623.

Farmer, D. M., Vagle, S., & Booth, A. D. (1998). A free-flooding acoustical resonator for measurement of bubble size distributions. *Journal of Atmospheric and Oceanic Technology, 15*, 1132–1146.

Hamme, R. C., Nicholson, D. P., Jenkins, W. J., & Emerson, S. R. (2019). Using noble gases to assess the ocean's carbon pumps. *Annual Review of Marine Science, 11*, 75–103.

Koweek, D. A., Mucciarone, D. A., & Dunbar, R. B. (2016). Bubble stripping as a tool to reduce high dissolved CO2 in coastal marine ecosystems. *Environmental Science & Technology, 50*(7), 3790–3797.

Lamarre, E., & Melville, W. K. (1991). Air entrainment and dissipation in breaking waves. *Nature, 351*, 469–472.

Leifer, I., & Patro, R. K. (2002). The bubble mechanism for methane transport from the shallow sea bed to the surface: A review and sensitivity study. *Continental Shelf Research, 22*, 2409–2428.

Liang, J.-H., McWilliams, J. C., Sullivan, P. P., & Baschek, B. (2011). Modeling bubbles and dissolved gases in the ocean. *Journal of Geophysical Research, 116*, C03015.

Liang, J.-H., McWilliams, J. C., Sullivan, P. P., & Baschek, B. (2012). Large eddy simulation of the bubbly ocean: New insights on subsurface bubble distribution and bubble-mediated gas transfer. *Journal of Geophysical Research, 117*, C04002. https://doi.org/10.1029/2011JC007766.

Liang, J.-H., Deutsch, C., McWilliams, J. C., Baschek, B., Sullivan, P. P., & Chiba, D. (2013). Parameterizing bubble-mediated air-sea gas exchange and its effect on ocean ventilation. *Global Biogeochemical Cycles, 27*, 894–905. https://doi.org/10.1002/gbc.20080.

Liang, J.-H., Emerson, S. R., D'Asaro, E. A., McNeil, C. L., Harcourt, R. R., Sullivan, P. P., Yang, B., & Cronin, M. F. (2017). On the role of sea-state in bubble-mediated air-sea gas flux during a winter storm. *Journal of Geophysical Research, Oceans, 122*, 2671–2685. https://doi.org/10.1002/2016JC012408.

Liss, P. S., & Slater, P. G. (1974). Flux of gases across the air-sea interface. *Nature, 247*, 181–184.

McNeil, C., & Asaro, E. D. (2007). Parameterization of air-sea gas fluxes at extreme wind speeds. *Journal of Marine Systems, 66*, 110–121.

McWilliams, J. C., Sullivan, P. P., & Moeng, C.-H. (1997). Langmuir turbulence in the ocean. *Journal of Fluid Mechanics, 334*, 1–30.

Melville, W. K., & Matusov, P. (2002). Distribution of breaking waves at the ocean surface. *Nature, 417*, 58–63.

Memery, L., & Merlivat, L. (1985). Modelling of gas flux through bubbles at the air-water interface. *Tellus B, 37*, 272–285.

Monahan, E. C., Spiel, D. E., & Davidson, K. L. (1986). A model of marine aerosol generation via whitecaps and wave disruption. In E. C. Monahan and G. Mac Niocaill, (Eds.), *Oceanic Whitecaps* (pp. 167–174). D. Reidel.

Monahan, E. C., & Torgersen, T. (1991). Enhancement of air-sea gas exchange by oceanic whitecapping. In S. C. Wilhelms & J. S. Gulliver (Eds.), *Air-water mass transfer: Selected papers from the second international symposium on gas transfer at water surfaces* (pp. 608–617). New York: American Society of Civil Engineers.

Nicholson, D. P., Emerson, S. R., Khatiwala, S., and Hamme, R. C. (2011). An inverse approach to estimate bubble-mediated air-sea gas flux from inert gas measurements. In *The 6th international symposium on gas transfer at water surfaces* (pp. 223–237). Kyoto University Press.

Nicholson, D. P., Khatiwala, S., & Heimbach, P. (2016). Noble gas tracers of ventilation during deep-water formation in the Weddell Sea. *IOP Conference Series: Earth and Environmental Science, 35*(1), 012019.

Shi, F., Kirby, J. T., & Ma, G. (2010). Modeling quiescent phase transport of air bubbles induced by breaking waves. *Ocean Modell, 35*, 105–117. https://doi.org/10.1016/j.ocemod.2010.07.002.

Stanley, R. H. R., W. J. Jenkins, D. E. Lott III, & S. C. Doney (2009) Noble gas constraints on air-sea gas exchange and bubble fluxes, Journal of Geophysical Research, 114, C11020.

Sullivan, P. P., & McWilliams, J. C. (2010). Dynamics of winds and currents coupled to surface waves. *Annual Review of Fluid Mechanics, 42*, 19–42.

Thorpe, S. A. (1982). On the clouds of bubbles formed by breaking wind-waves in deep water, and their role in air-sea gas transfer. *Philosophical Transaction of the Royal Society London A, 304*, 155–210.

Vagle, S., McNeil, C., & Steiner, N. (2010). Upper ocean bubble measurements from the NE pacific and estimates of their role in air-sea gas transfer of the weakly soluble gases nitrogen and oxygen. *Journal of Geophysical Research, 115*, C12054.

Vlahos, P., & Monahan, E. C. (2009). A generalized model for the air-sea transfer of dimethyl sulfide at high wind speeds. *Geophysical Research Letters, 36*, L21605.

Vlahos, P., Monahan, E. C., Huebert, B. J., & Edson, J. B. (2011). Wind-dependence of dms transfer velocity: Comparison of model with recent southern ocean observations. In *The 6th international symposium on gas transfer at water surfaces* (pp. 455–463). Kyoto University Press.

Wang, D. W., Wijesekera, H. W., Jarosz, E., Teague, W. J., & Pegau, W. S. (2016). Turbulent diffusivity under high winds from acoustic measurements of bubbles. *Journal of Physical Oceanography, 46*, 1593–1613.

Wanninkhof, R., Asher, W. E., Ho, D. T., Sweeney, C., & McGillis, W. R. (2009). Advances in quantifying air-sea gas exchange and environmental forcing. *Annual Review of Marine Science, 1*, 213–244.

Wanninkhof, R., Asher, W., Weppernig, R., Chen, H., Schlosser, P., Langdon, C., & Sambrotto, R. (1993). Gas transfer experiment on Georges Bank using two volatile deliberate tracers. *Journal of Geophysical Research, 98*, 20237–20248.

Woolf, D. K. (1997). Bubbles and their role in gas exchange. In P. S. Liss & R. A. Duce (Eds.), *The Sea Surface and Global Change* (pp. 173–206). Cambridge: Cambridge Univ. Press.

Woolf, D. K., & Thorpe, S. A. (1991). Bubbles and the air-sea exchange of gases in near-saturation conditions. *Journal of Marine Research, 49*, 435–466.

Zhao, Z., D'Asaro, E. A., & Nystuen, J. A. (2014). The sound of tropical cyclones. *Journal of Physical Oceanography, 44*, 2763–2778.